Figure S1

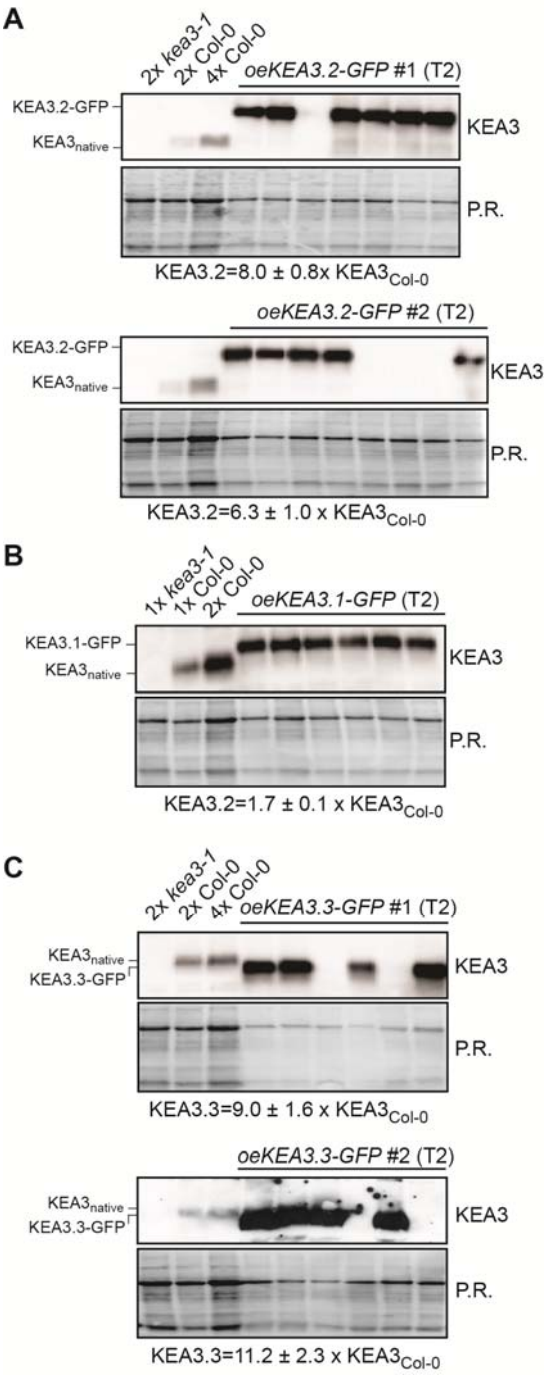

Fig. S1: Segregation analysis and quantification of KEA3 levels in overexpressing lines. Leaves of segregating overexpression lines of *KEA3.2-GFP* (*oeKEA3.2*) (A), *KEA3.1-GFP* (*oeKEA3.1*) (B) and *KEA3.3-GFP* (*oeKEA3.3*) (C) in the *kea3-1* background (T2 generation) were analyzed for presence and levels of KEA3 by immunoblot analysis. The average protein level of a line was calculated from the specific KEA3 signal of plants that expressed KEA3 proteins normalized to their Ponceau Red (P.R.) signal. Plants overexpressing the *KEA3* constructs were then analyzed to generate Fig. 2.

Figure S2

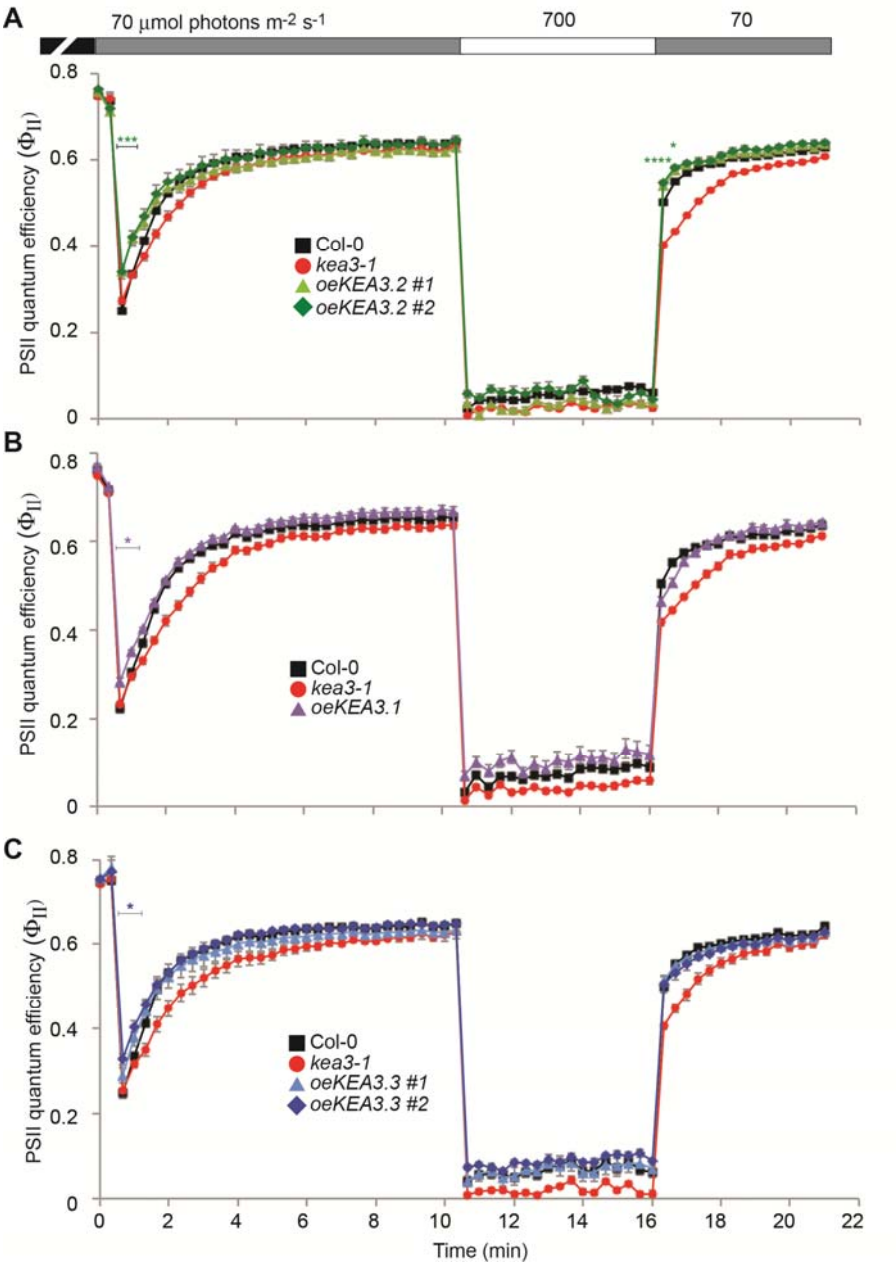

Fig. S2 Overexpression of the different *KEA3* splice forms reveals isoform-specific properties. Full traces of PSII quantum efficiency (Φ_{II}) from experiments shown in Fig 2. In detail chlorophyll fluorescence of detached, dark-acclimated leaves from Col-0, *kea3-1* and *kea3-1* overexpressing *KEA3.2-GFP* (*oeKEA3.2*) (A), *KEA3.1-GFP* (*oeKEA3.1*) (B), and *KEA3.3-GFP* (*oeKEA3.3*) (C) was monitored during alternating low light (70 µmol photons m^{-2} s^{-1}, grey bar), high light (700 µmol photons m^{-2} s^{-1}, white bar) and low light and PSII quantum efficiency was calculated. Asterisks indicate where PSII quantum efficiency is significantly higher in all measured lines of one construct as compared to Col-0 (*0.01<*P*<0.05, ***0.001<*P*<0.005, ****P<0.001, one-way ANOVA with Tukey's *post hoc* test). Error bars represent SEM (n=4-6).

Figure S3

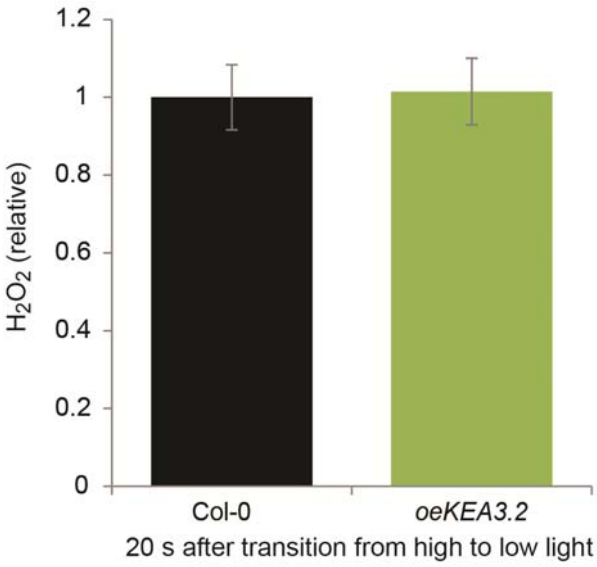

Fig. S3 The Mehler reaction product H_2O_2 is not significantly higher in *oeKEA3.2* after shift from high to low light, when Φ_{II} is increased. Leaf H_2O_2 content was determined using the Amplex Red assay and expressed as resorufin fluorescence against a standard curve. Results were normalized to chlorophyll. Data are expressed relative to the WT average. Error bars represent SEM (n=6).

Figure S4

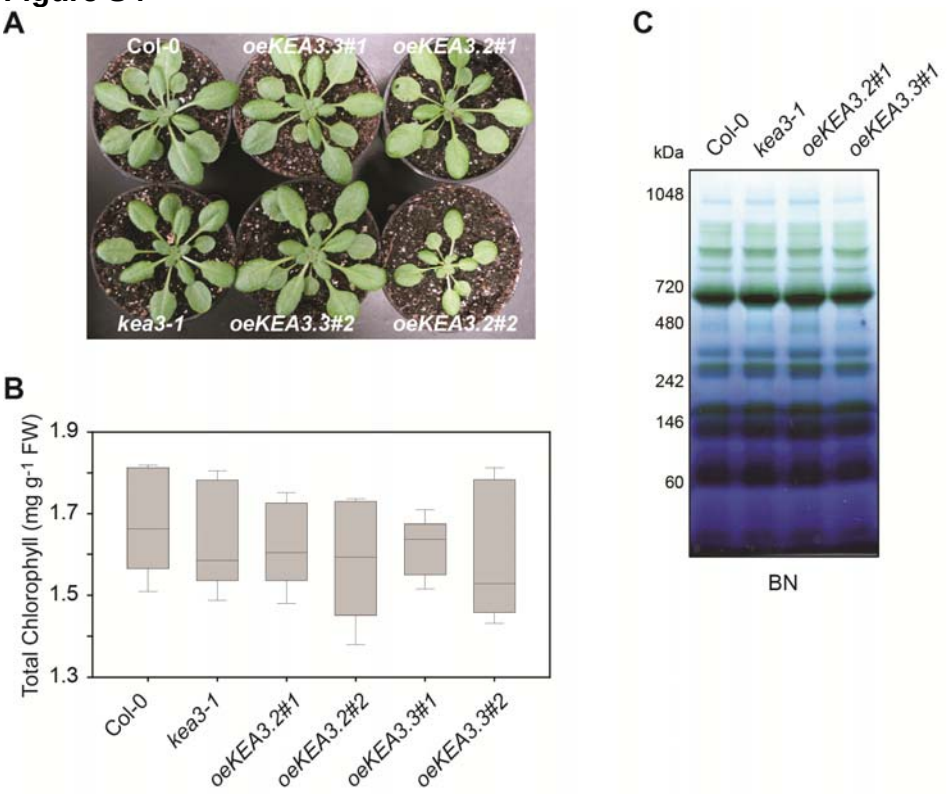

Fig. S4 Growth, pigmentation and levels of photosynthetic complexes appear unchanged in *oeKEA3.2* and *oeKEA3.3* grown in low light. (A) 35-day old Col-0, *kea3-1*, *oeKEA3.2* and *oeKEA3.3* plants were imaged (*oeKEA3.2*#2 showed delayed germination). (B) Chlorophyll content was determined (error bars represent SEM, n=6). (C) Thylakoids were isolated, complexes were solubilized with 0.7 % n-dodecyl-β-D-maltoside and proteins were separated by Blue-native (BN)-PAGE.

Figure S5

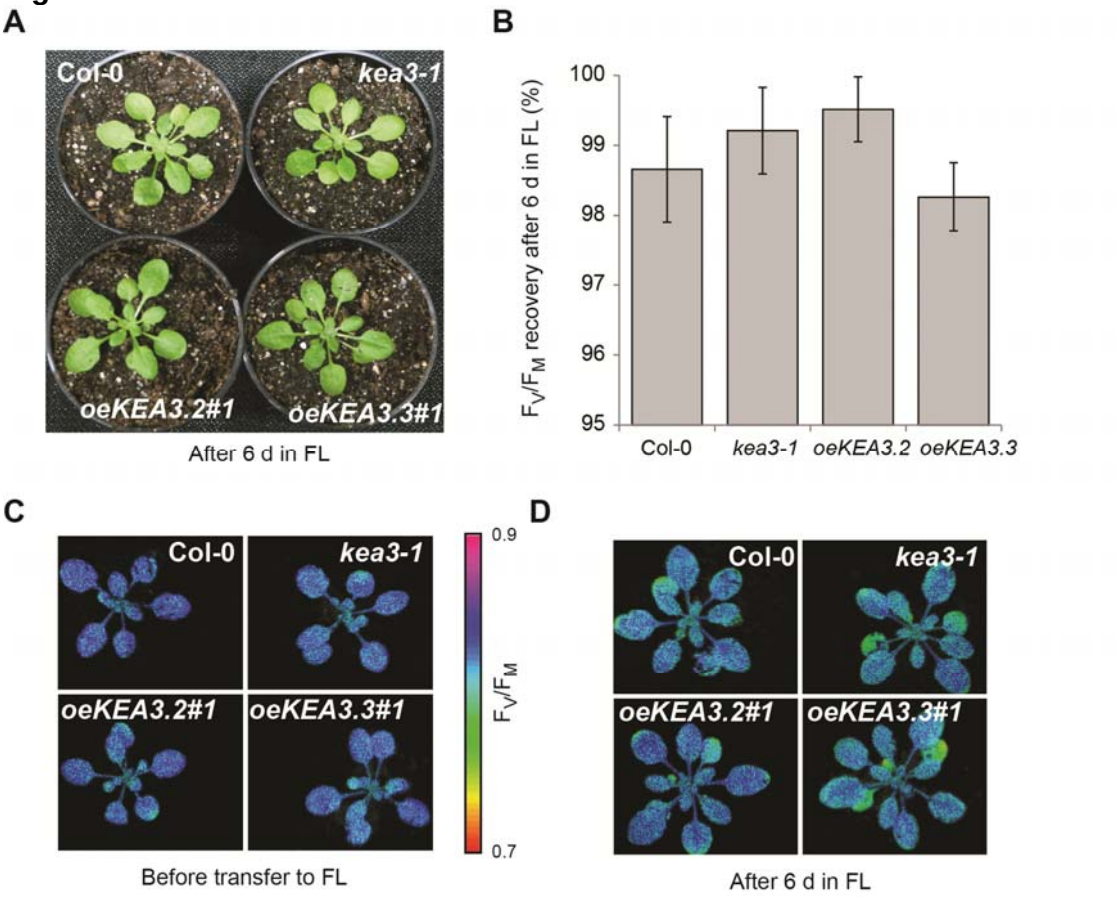

Fig. S5 Analyses of growth and photosynthetic efficiency in fluctuating light (FL). (A) 5-week-old Col-0, *kea3-1*, *oeKEA3.2*#1 and *oeKEA3.3*#1 after shift to fluctuating high and low light conditions for six days (1 min 900 µmol photons m^{-2} s^{-1}, 5 min 90 µmol photons m^{-2} s^{-1}). (B) F_v/F_m recovery of plants shifted from 150 µmol photons m^{-2} s^{-1} to fluctuating light after six days as compared to before the treatment. (C,D) False color images representing F_v/F_m values of Col-0, *kea3-1*, *oeKEA3.2* and *oeKEA3.3* before (C) and six days after the shift to FL.

Figure S6

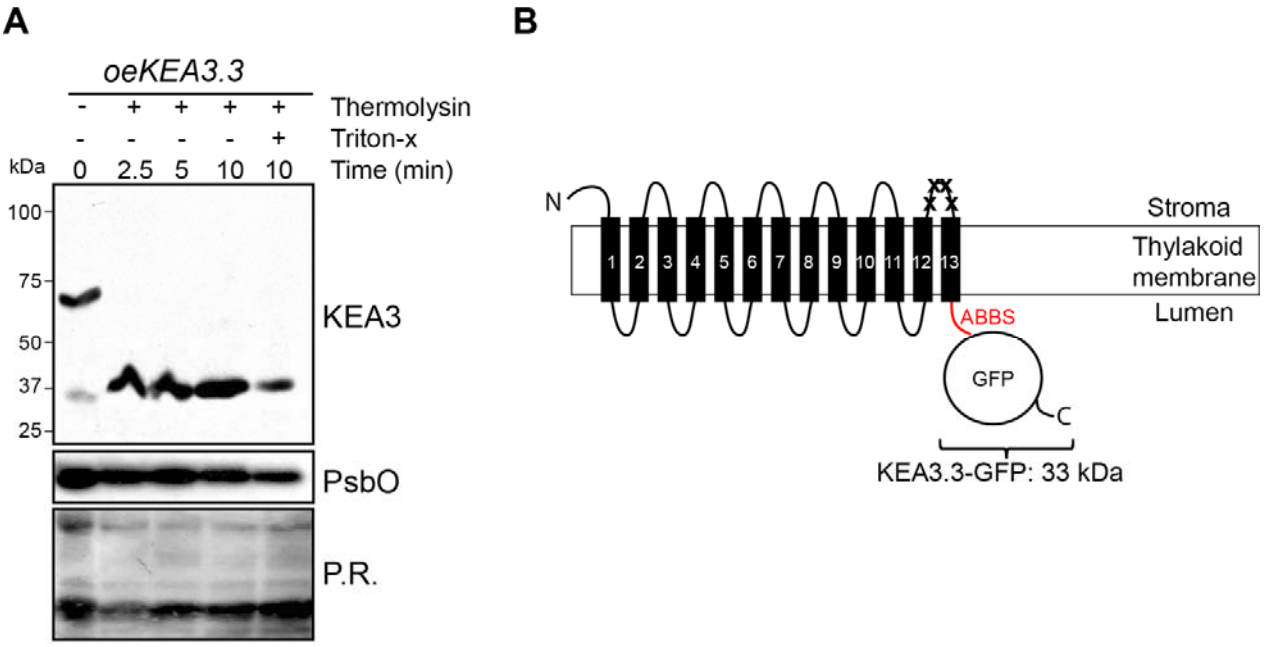

Fig. S6 The C-terminus of KEA3.3 is localized in the thylakoid lumen. (A) Intact thylakoids of *oeKEA3.3* were treated with thermolysin in the absence and presence of Triton-X. Aliquots were removed at the specified time points, separated by SDS-PAGE and immunodetection of KEA3 and PsbO was performed. Prior to immunodetection, membranes were stained with Ponceau Red (P.R.). (B) Schematic overview of the KEA3 topology resulting from the thermolysin treatment. The antibody binding site (ABBS, red, containing 5 thermolysin sites) present in the C-terminus is protected from thermolysin treatment. Crosses mark stroma-accessible thermolysin sites close to the antibody-binding site.

Figure S7

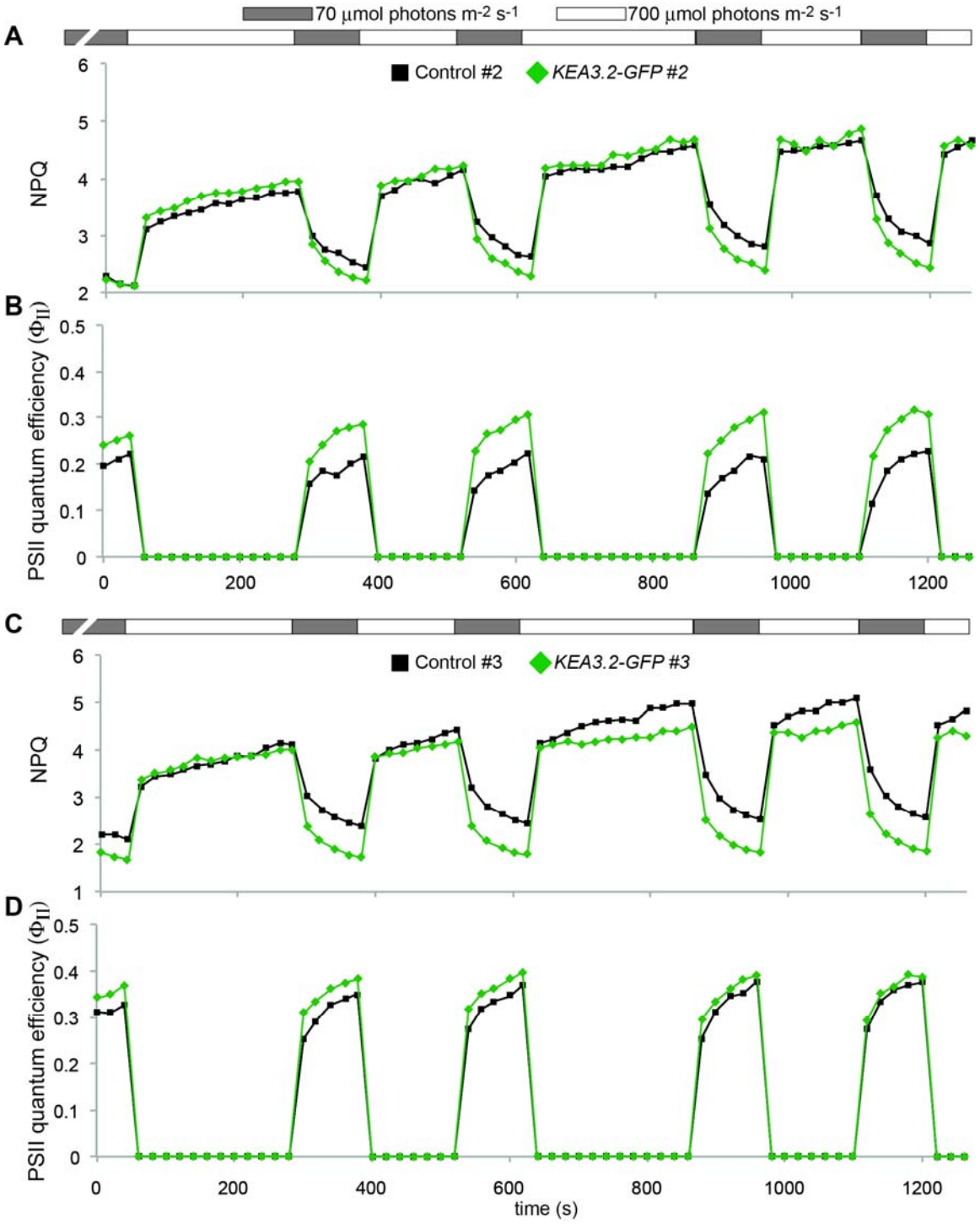

Fig. S7: Overexpression of *KEA3.2* in tobacco enhances photosynthetic yield in fluctuating light**.** (A-D) Chlorophyll fluorescence of tobacco leaves transformed with either *KEA3.2-GFP* or *GFP* fused to the KEA3 antibody-binding site coding sequence at its N-terminus (control) was monitored under fluctuating high light (1000 µmol photons m^{-2} s^{-1}, white bar) and low light (70 µmol photons m^{-2} s^{-1}, grey bar) and NPQ (A,C) and PSII quantum efficiency (B,D) were calculated. Traces are from independent experiments.

Figure S8

A

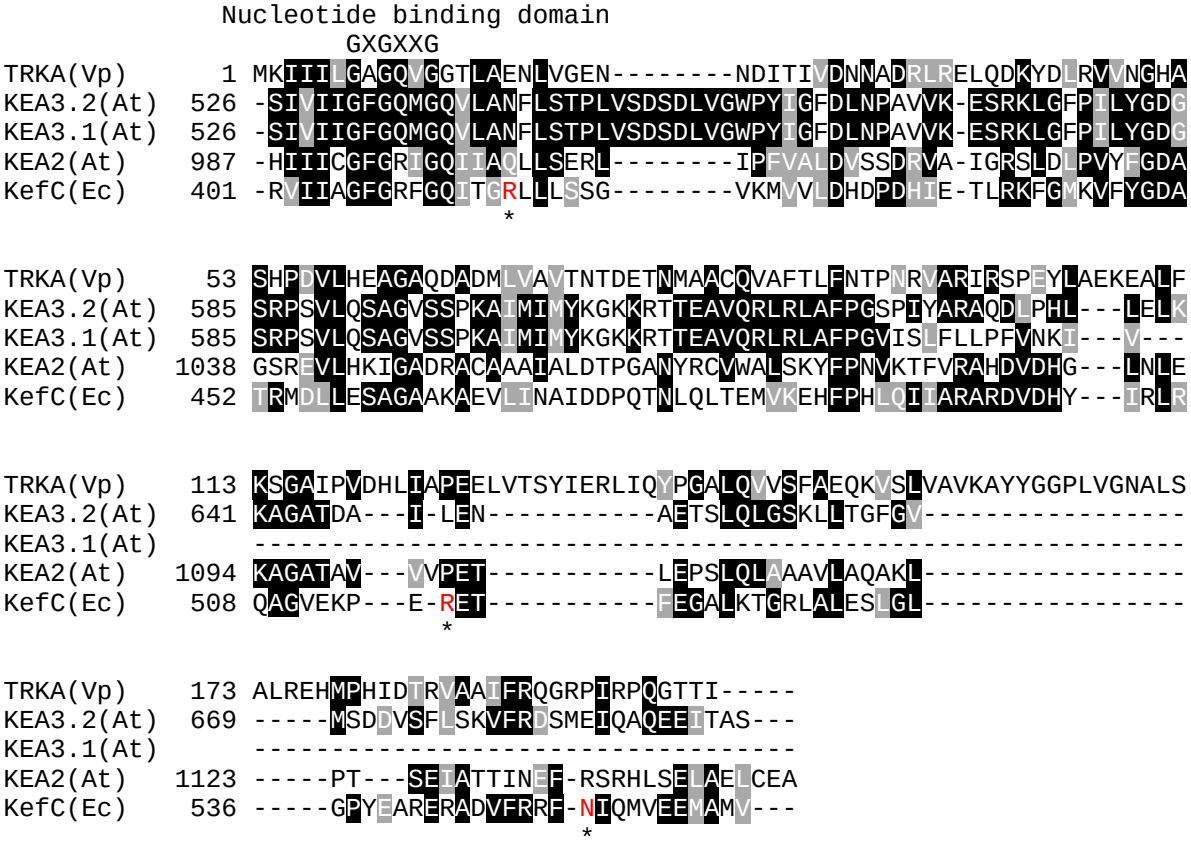

B

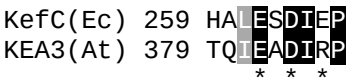

Fig. S8: Alignments of KTN domains and transmembrane gating structures. (A) KTN domains of KEA3.1, KEA3.2 and KEA2 from *Arabidopsis* (At), KefC from *E.coli* (Ec) and TrkA from *V. parahaemolyticus* (Vp) were aligned using ClustalOmega and shaded according to similarity with the box-shade server. The GXGXXG marks the Rossman fold nucleotide binding domain. Amino acids that confer glutathione binding to the KefC KTN domain are marked in red and by asterisks. (B) The transmembrane gating structure of KefC was aligned with the homologous region of KEA3. Asterisks indicate the three acidic amino acid residues of KefC, which are critical for interaction of this structure with the KTN domain (Ness and Booth 1999; Roosild et al. 2002).